The Theory of
Plasma Wakefield Acceleration (beam driven)
and various novel methods

Dr Öznur Mete Apsimon
The University of Lancaster
The Cockcroft Institute of Accelerator Science and Technology

Introduction

S. Livingstone'ın hazırladığı çizelgeden güncelleştirilmiştir.

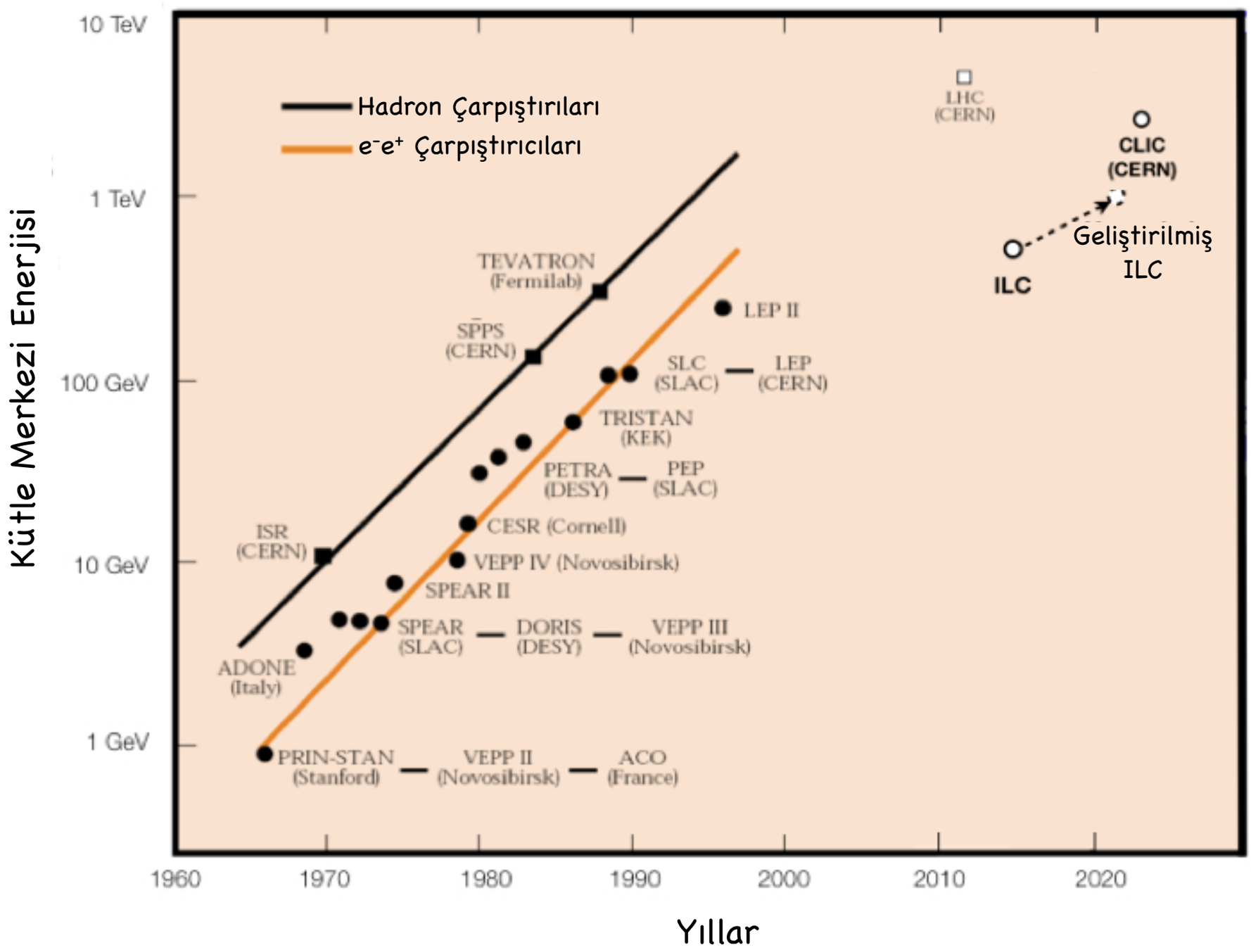

Normal iletken metalik teknolojinin limiti

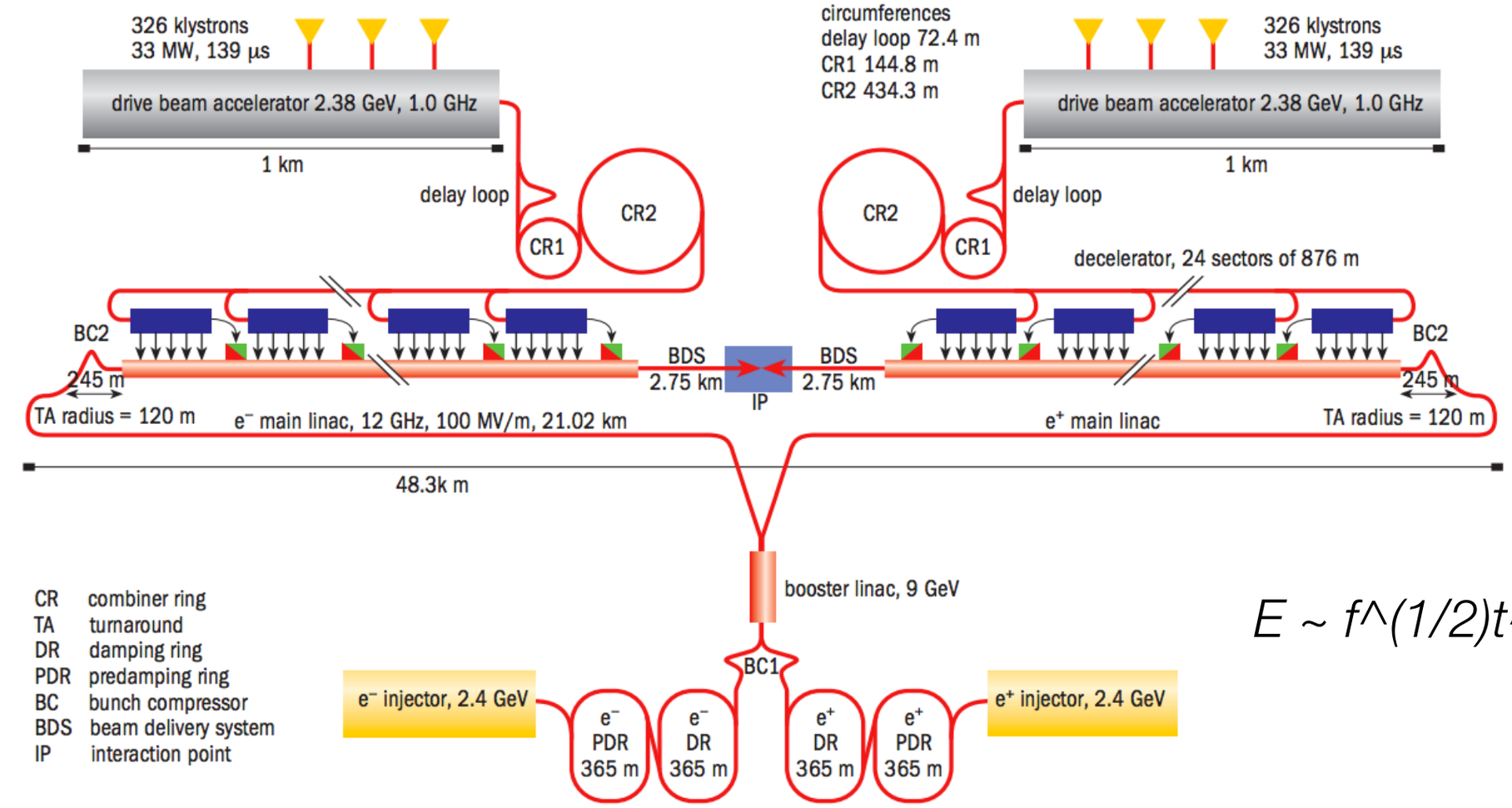

$E \sim f^{1/2} t^{-1/4}$

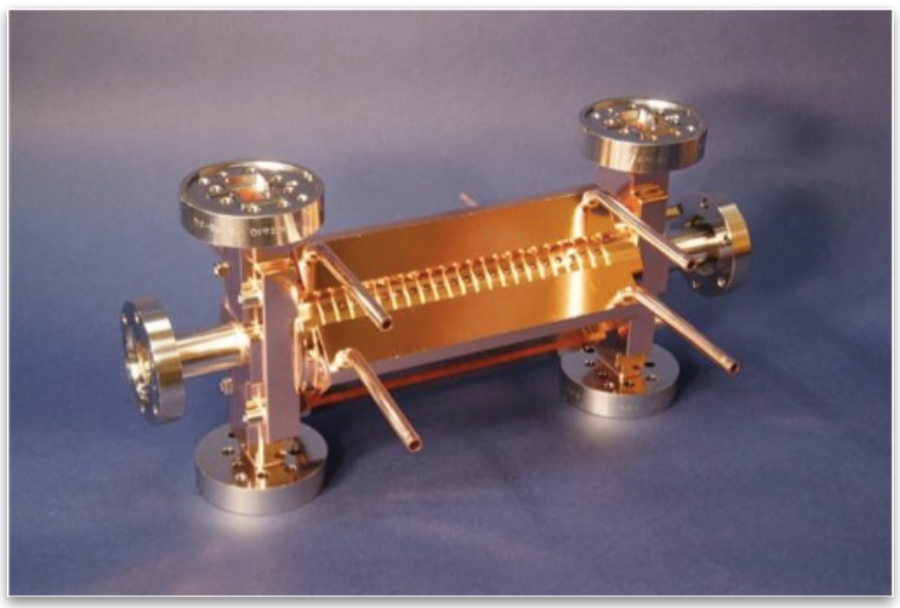

100 MV/m, 12 GHz

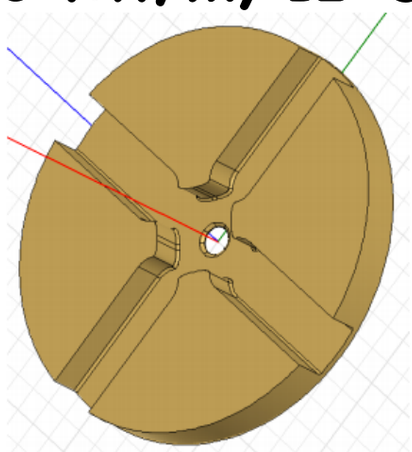

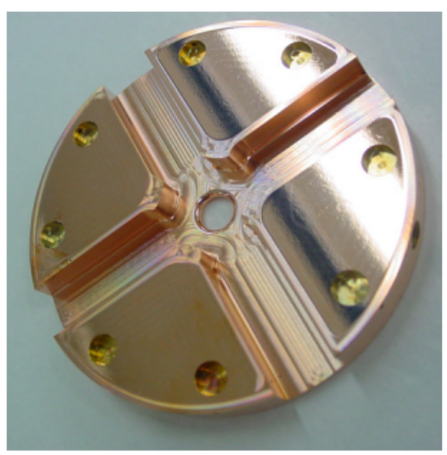

Introduction

We need novel methods to build next generation colliders with resonable budgets and sizes.

Main topic:

- Acceleration in laser or particle driven plasma wake fields,

Other advanced acceleration schemes

- Dielectric acceleration driven by a laser,
- Terahertz acceleration, acceleration by laser electric field.

Contents

In this lecture…

- Terahertz-driven accelerators
- Dielectric accelerators
- What is plasma?
- Laser driven plasma accelerators
- Beam-driven plasma acceleration derivation example:
  The wakefield response in the plasma
- Proton-driven plasma acceleration, self modulation instability
- Positron acceleration, use of hollow plasma channel

Terahertz Accelerators

nature COMMUNICATIONS

ARTICLE

Received 20 Apr 2015 | Accepted 27 Aug 2015 | Published 6 Oct 2015

DOI: 10.1038/ncomms9486 OPEN

Terahertz-driven linear electron acceleration

Emilio A. Nanni[1], Wenqian R. Huang[1], Kyung-Han Hong[1], Koustuban Ravi[1], Arya Fallahi[2,3], Gustavo Moriena[4], R.J. Dwayne Miller[3,4,5] & Franz X. Kärtner[1,2,3,6]

The cost, size and availability of electron accelerators are dominated by the achievable accelerating gradient. Conventional high-brightness radio-frequency accelerating structures operate with 30–50 MeV m^{-1} gradients. Electron accelerators driven with optical or infrared sources have demonstrated accelerating gradients orders of magnitude above that achievable with conventional radio-frequency structures. However, laser-driven wakefield accelerators require intense femtosecond sources and direct laser-driven accelerators suffer from low bunch charge, sub-micron tolerances and sub-femtosecond timing requirements due to the short wavelength of operation. Here we demonstrate linear acceleration of electrons with keV energy gain using optically generated terahertz pulses. Terahertz-driven accelerating structures enable high-gradient electron/proton accelerators with simple accelerating structures, high repetition rates and significant charge per bunch. These ultra-compact terahertz accelerators with extremely short electron bunches hold great potential to have a transformative impact for free electron lasers, linear colliders, ultrafast electron diffraction, X-ray science and medical therapy with X-rays and electron beams.

Terahertz-Driven Accelerators

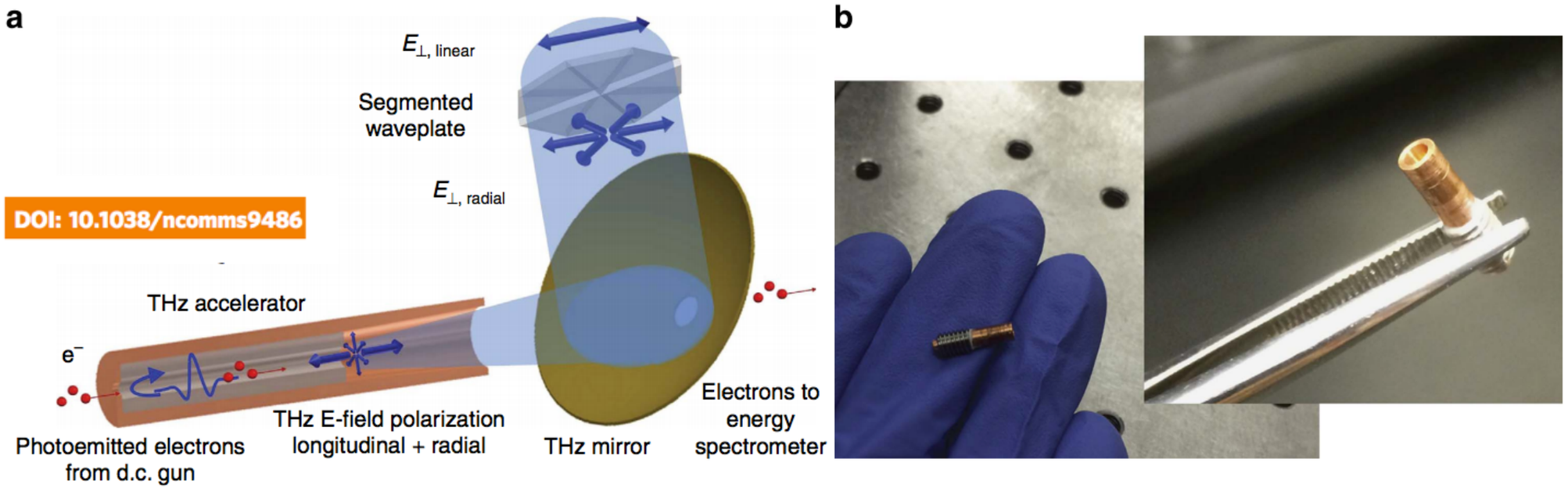

Figure 1 | Terahertz-driven linear accelerator. (**a**) Schematic of the THz LINAC. Top right: a linearly polarized THz pulse is converted into a radially polarized pulse by a segmented waveplate before being focused into the THz waveguide. The THz pulse is reflected at the end of the waveguide to co-propagate with the electron bunch, which enters the waveguide through a pinhole (lower left). The electron bunch is accelerated by the longitudinal electric field of the co-propagating THz pulse. The electron bunch exits the THz waveguide and passes through a hole in the focusing mirror (right) for the THz pulse. (**b**) Photograph of the compact millimetre scale THz LINAC. (**c**) The time-domain waveform of the THz pulse determined with electro-optic sampling (see Methods: Electro-optic sampling). Insert: corresponding frequency-domain spectrum. (**d**) The time-domain waveform of the THz pulse at the exit of a THz waveguide 5 cm in length, including two tapers. (**e**) Normalized intensity of the focused THz beam.

Terahertz Accelerators

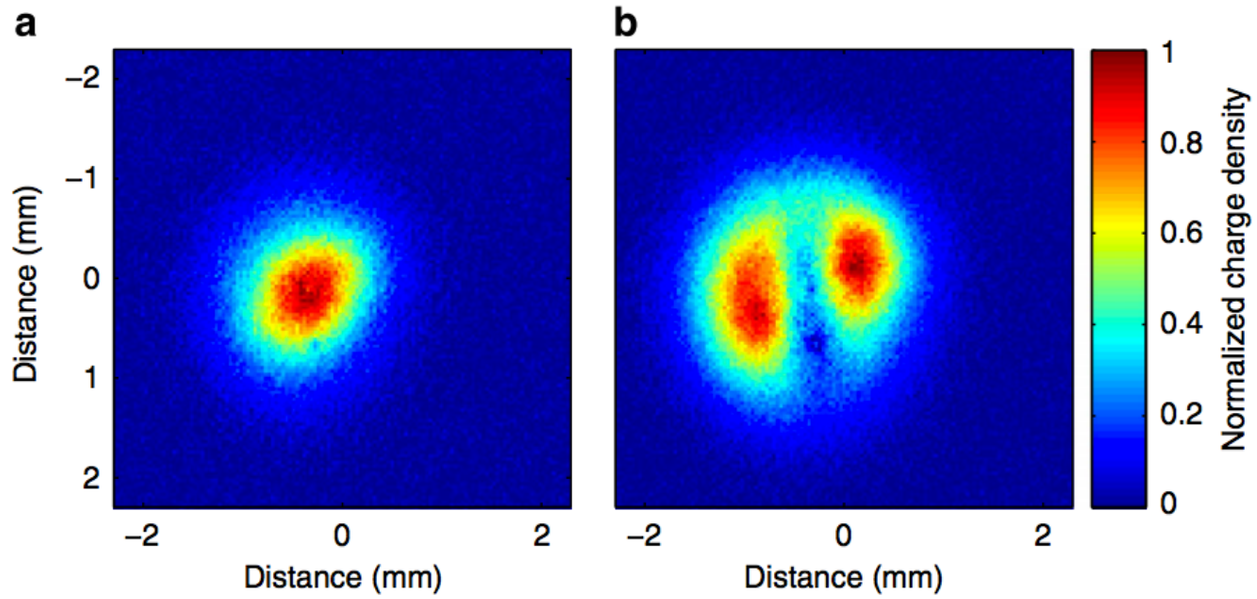

DOI: 10.1038/ncomms9486

Figure 2 | Demonstration of terahertz acceleration. Transverse electron density of the electron bunch as recorded by a micro-channel plate (MCP) at 59 kV for (**a**) THz off and (**b**) THz on. The bimodal distribution is due to the presence of accelerated and decelerated electrons, which are separated spatially by the magnetic dipole energy spectrometer. The images are recorded over a 3-s exposure at 1 kHz repetition rate. (**c**) Comparison between simulated (red) and measured (black) energy spectrum of the electron bunch measured at the MCP due to the deflection of the beam by a magnetic dipole. At 59 keV and with 25 fC per bunch, the simulation predicts a $\sigma_{\perp} = 513\,\mu m$ and $\Delta E = 1.25$ keV. The observed $\Delta E/E$ appears larger due to the large transverse size of the beam. After the pinhole, the transverse emittance is 25 nm rad and the longitudinal emittance is 5.5 nm rad. (**d**) Comparison between simulated (red) and measured (black) electron bunch at MCP after acceleration with THz. Decelerated electrons are present due to the long length of the electron bunch, as well as the slippage between the THz pulse and the electron bunch. Error bars in **c** and **d** correspond to one s.d. in counts over the data set of 10 integrated exposures.

Dielectric Accelerators

Accelerator on a Chip

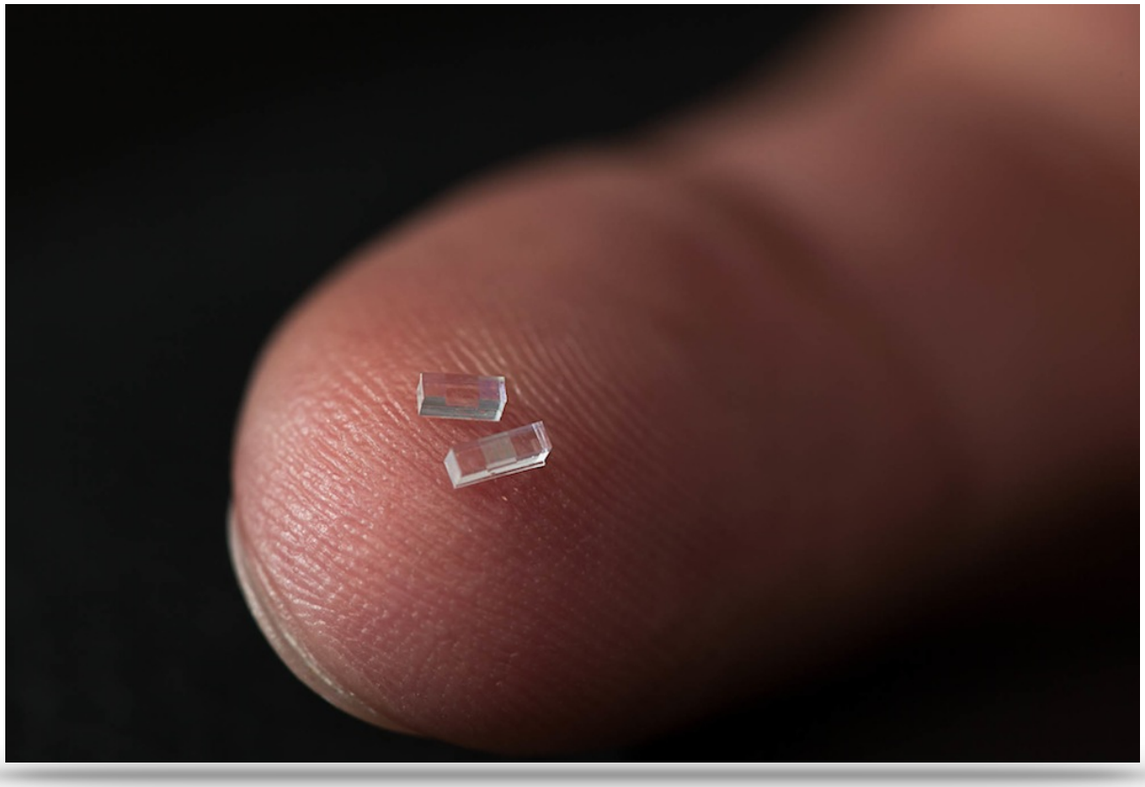

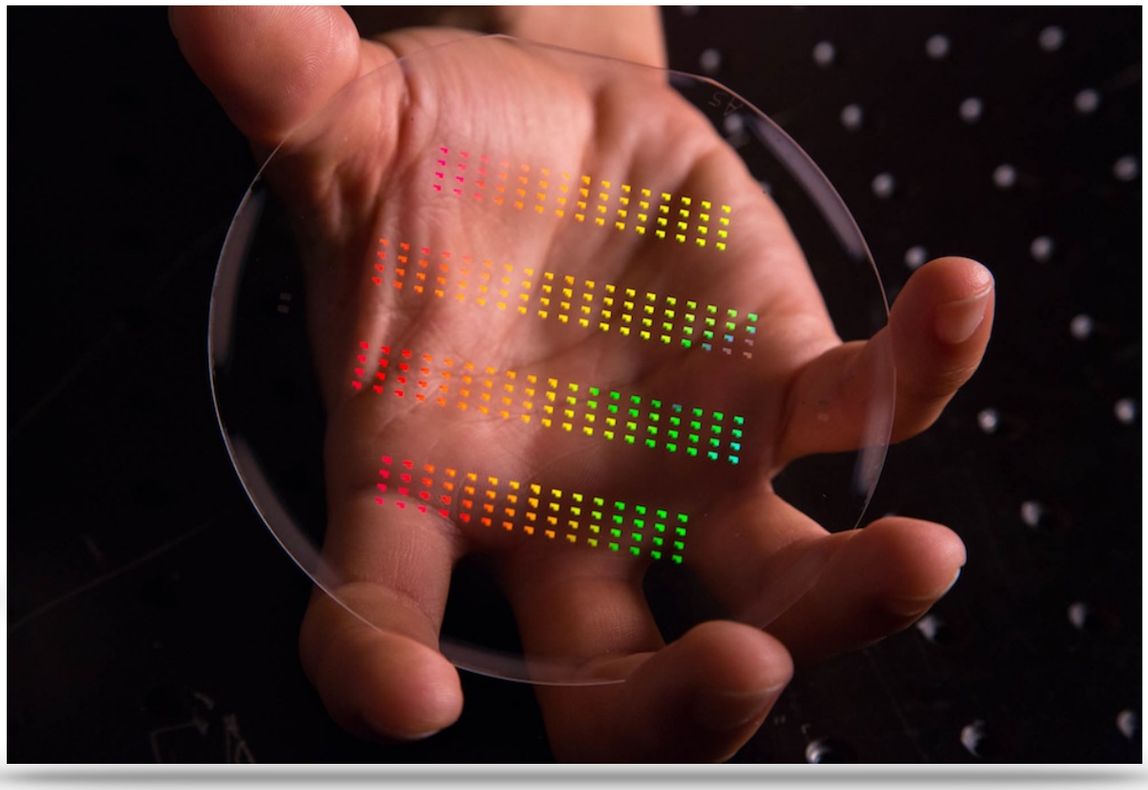

VIDEO
https://www6.slac.stanford.edu/news/2013-09-27-accelerator-on-a-chip.aspx

Dielectric Accelerators

LETTER

doi:10.1038/nature12664

Demonstration of electron acceleration in a laser–driven dielectric microstructure

E. A. Peralta[1], K. Soong[1], R. J. England[2], E. R. Colby[2], Z. Wu[2], B. Montazeri[3], C. McGuinness[1], J. McNeur[4], K. J. Leedle[3], D. Walz[2], E. B. Sozer[4], B. Cowan[5], B. Schwartz[5], G. Travish[4] & R. L. Byer[1]

The enormous size and cost of current state-of-the-art accelerators based on conventional radio-frequency technology has spawned great interest in the development of new acceleration concepts that are more compact and economical. Micro-fabricated dielectric laser accelerators (DLAs) are an attractive approach, because such dielectric microstructures can support accelerating fields one to two orders of magnitude higher than can radio-frequency cavity-based accelerators. DLAs use commercial lasers as a power source, which are smaller and less expensive than the radio-frequency klystrons that power today's accelerators. In addition, DLAs are fabricated via low-cost, lithographic techniques that can be used for mass production. However, despite several DLA structures having been proposed recently[1–4], no successful demonstration of acceleration in these structures has so far been shown. Here we report high-gradient (beyond

permanent magnet undulator limits the compactness of such a structure and introduces deleterious synchrotron radiation effects.

An alternative way to satisfy the phase-velocity condition is by creating tailored longitudinal modes in near-field structures. One such approach, the inverse Smith–Purcell accelerator[12], has been demonstrated using a metallic grating[13], and more recently, in a dielectric grating with a NIR laser[14]. In configurations that minimize the transverse forces, these open structures do not support speed-of-light longitudinal eigenmodes and are therefore useful only at sub-relativistic particle energies. Additionally, they produce an exponentially decaying accelerating field pattern, which distorts the beam. To address these issues, designs using waveguides and photonic crystals have been proposed[1–3]. These structures present challenging fabrication tolerances, and the required modes are difficult to excite efficiently; as a result, no success-

Dielectric Accelerators

Accelerator on a Chip

E. A. Peralta et al., Nature, 27 Sept 2013 (10.1038/nature12664)

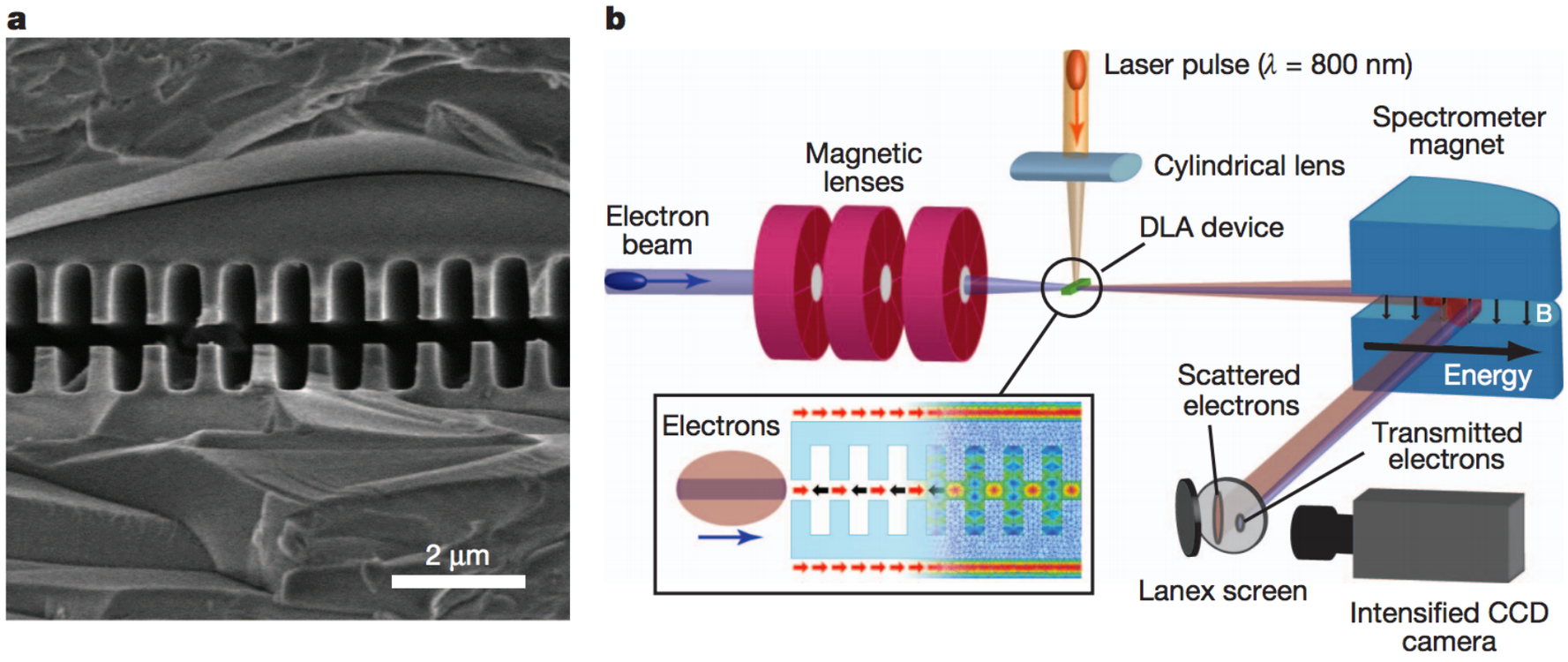

Figure 1 | DLA structure and experimental set-up. **a**, Scanning electron microscope image of the longitudinal cross-section of a DLA structure fabricated as depicted in Extended Data Fig. 1a. Scale bar, 2 μm. **b**, Experimental set-up. Inset, a diagram of the DLA structure indicating the field polarization direction and the effective periodic phase reset, depicted as alternating red (acceleration) and black (deceleration) arrows. A snapshot of the simulated fields in the structure shows the corresponding spatial modulation in the vacuum channel. See text for details.

Dielectric Accelerators

Accelerator on a Chip

E. A. Peralta et al., Nature, 27 Sept 2013 (10.1038/nature12664)

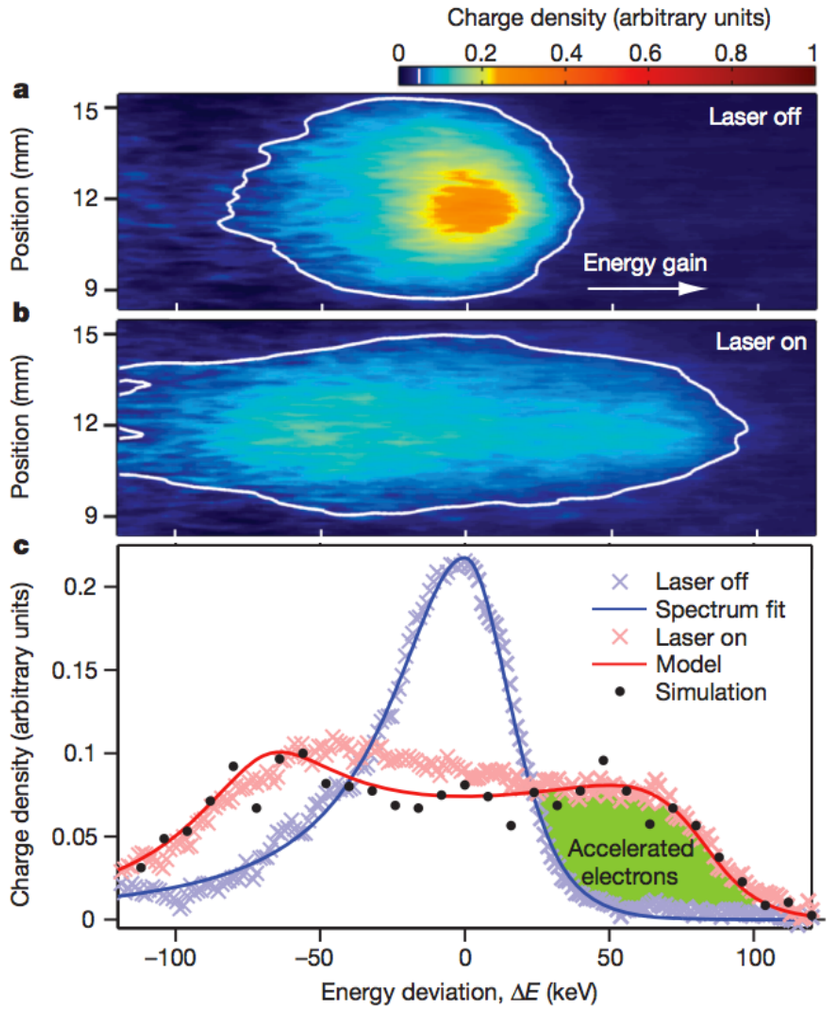

Figure 2 | Demonstration of energy modulation. **a**, Image of the transmitted electron beam on the spectrometer screen, with the laser off. **b**, As **a** but when the laser field is present. **c**, Energy spectra from **a** and **b** showing energy modulation. A fit (blue curve) to the measured laser-off spectrum (light blue crosses) is used as input for the simulations. The calculated energy modulation (red curve) and particle tracking simulations (black dots) agree with our measured spectrum (pink crosses). Images of the entire spectrometer screen are shown in Extended Data Fig. 2.

implies 151.2 MV/m

Plasma Accelerators

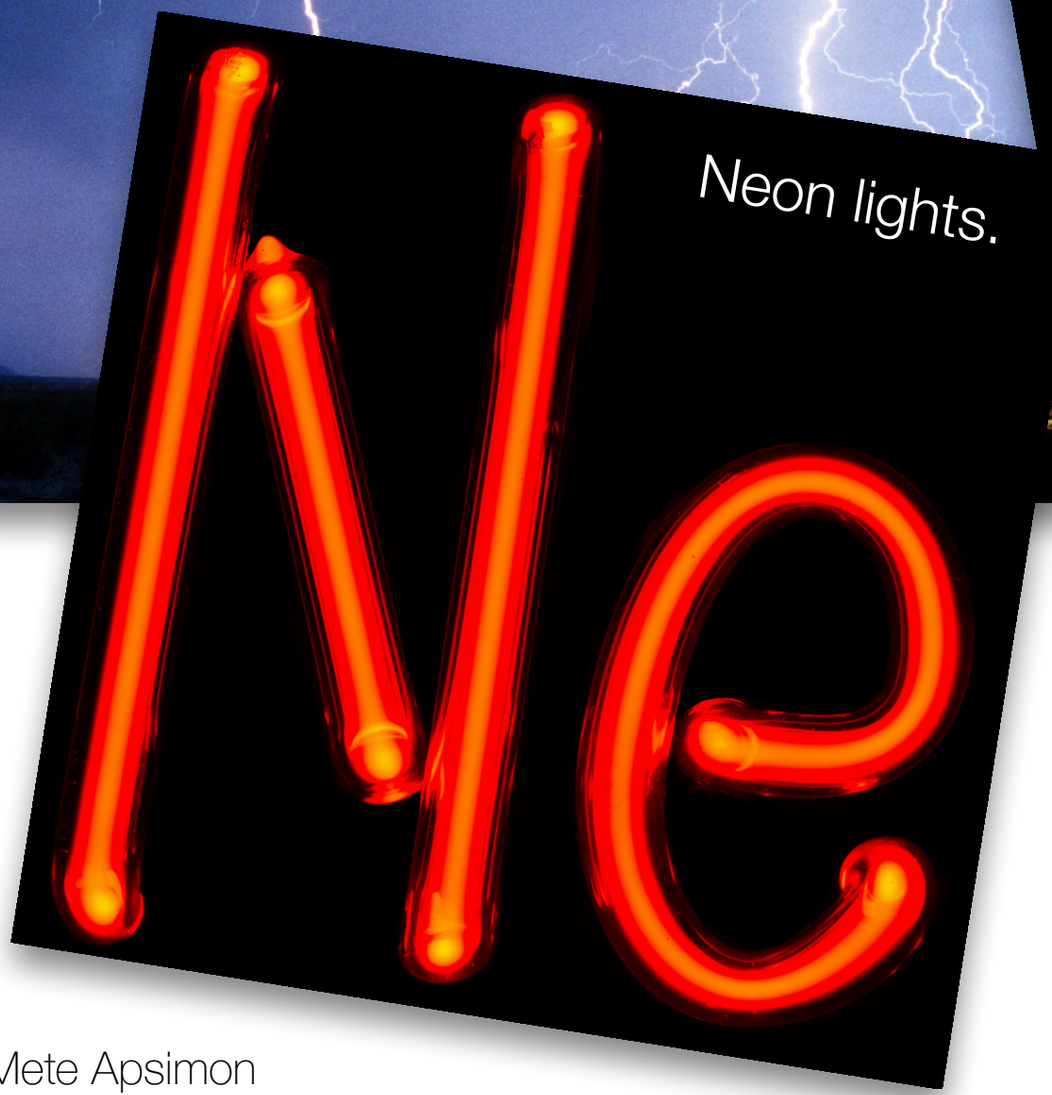

Introduction

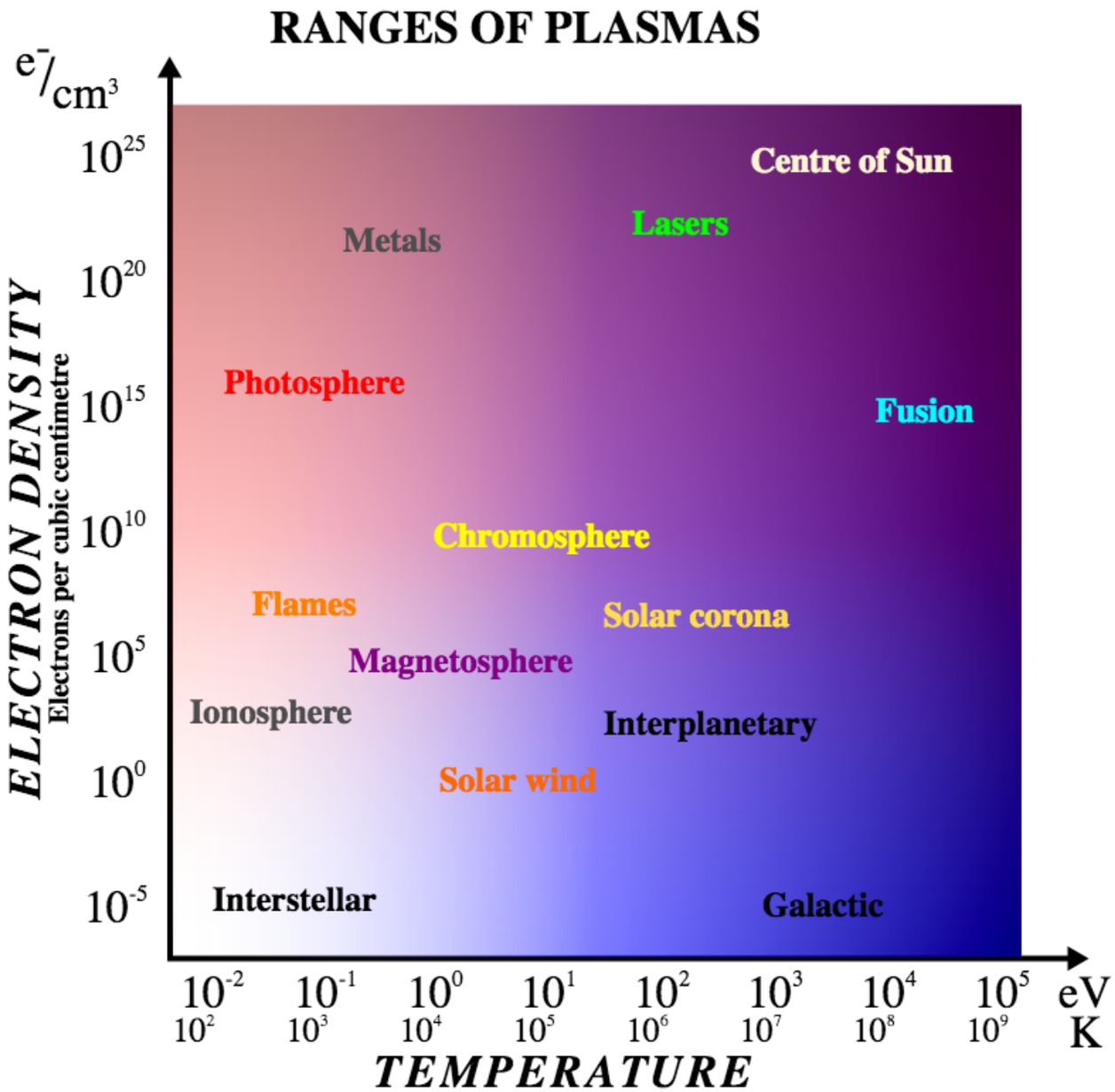

Peratt, A. L. (1996). "Advances in Numerical Modeling of Astrophysical and Space Plasmas". Astrophysics and Space Science 242 (1–2): 93–163.

Introduction

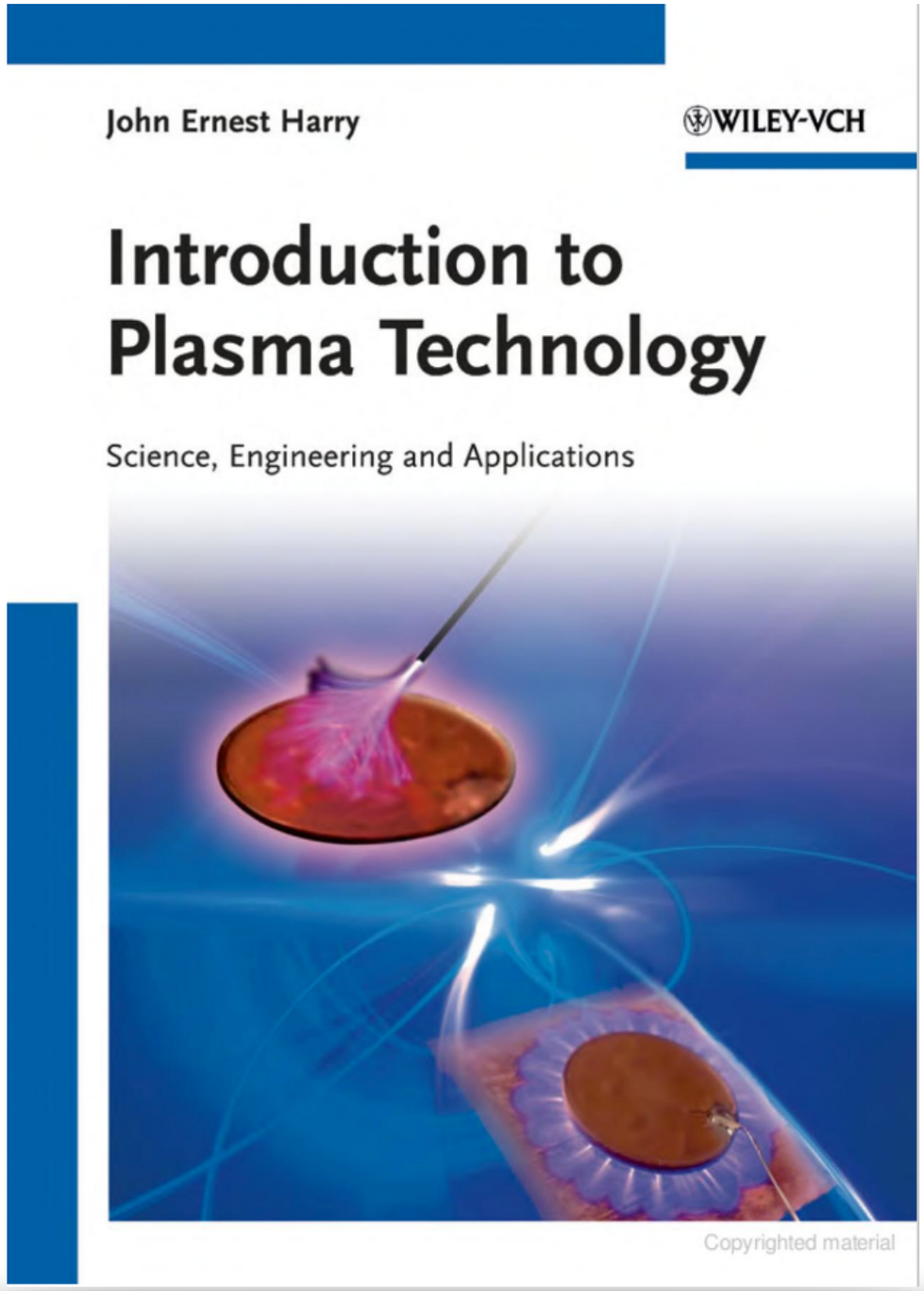

Introduction

- Plazma elektronları denge noktası çevresinde ω_p frekansında salınım yaparlar.

$$\omega_p = \sqrt{\frac{n_p e^2}{\epsilon_0 m}}$$

- Debye uzunluğu

$$\lambda_d = \sqrt{\frac{\epsilon_0 k_b T_e}{n_e e^2}}$$

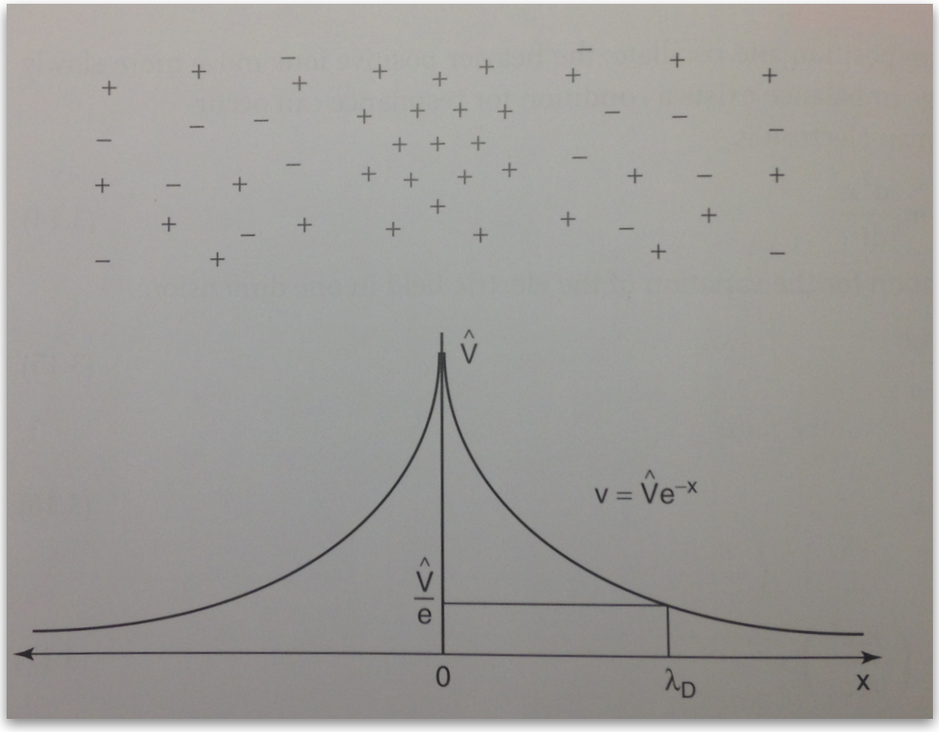

Laser Driven PWA

REVIEWS OF MODERN PHYSICS, VOLUME 81, JULY–SEPTEMBER 2009

Physics of laser-driven plasma-based electron accelerators

E. Esarey, C. B. Schroeder, and W. P. Leemans

Lawrence Berkeley National Laboratory, Berkeley, California 94720, USA

(Published 27 August 2009)

Laser-driven plasma-based accelerators, which are capable of supporting fields in excess of 100 GV/m, are reviewed. This includes the laser wakefield accelerator, the plasma beat wave accelerator, the self-modulated laser wakefield accelerator, plasma waves driven by multiple laser pulses, and highly nonlinear regimes. The properties of linear and nonlinear plasma waves are discussed, as well as electron acceleration in plasma waves. Methods for injecting and trapping plasma electrons in plasma waves are also discussed. Limits to the electron energy gain are summarized, including laser pulse diffraction, electron dephasing, laser pulse energy depletion, and beam loading limitations. The basic physics of laser pulse evolution in underdense plasmas is also reviewed. This includes the propagation, self-focusing, and guiding of laser pulses in uniform plasmas and with preformed density channels. Instabilities relevant to intense short-pulse laser-plasma interactions, such as Raman, self-modulation, and hose instabilities, are discussed. Experiments demonstrating key physics, such as the production of high-quality electron bunches at energies of 0.1–1 GeV, are summarized.

DOI: 10.1103/RevModPhys.81.1229 PACS number(s): 52.38.Kd, 41.75.Lx, 52.40.Mj

Laser Driven PWA

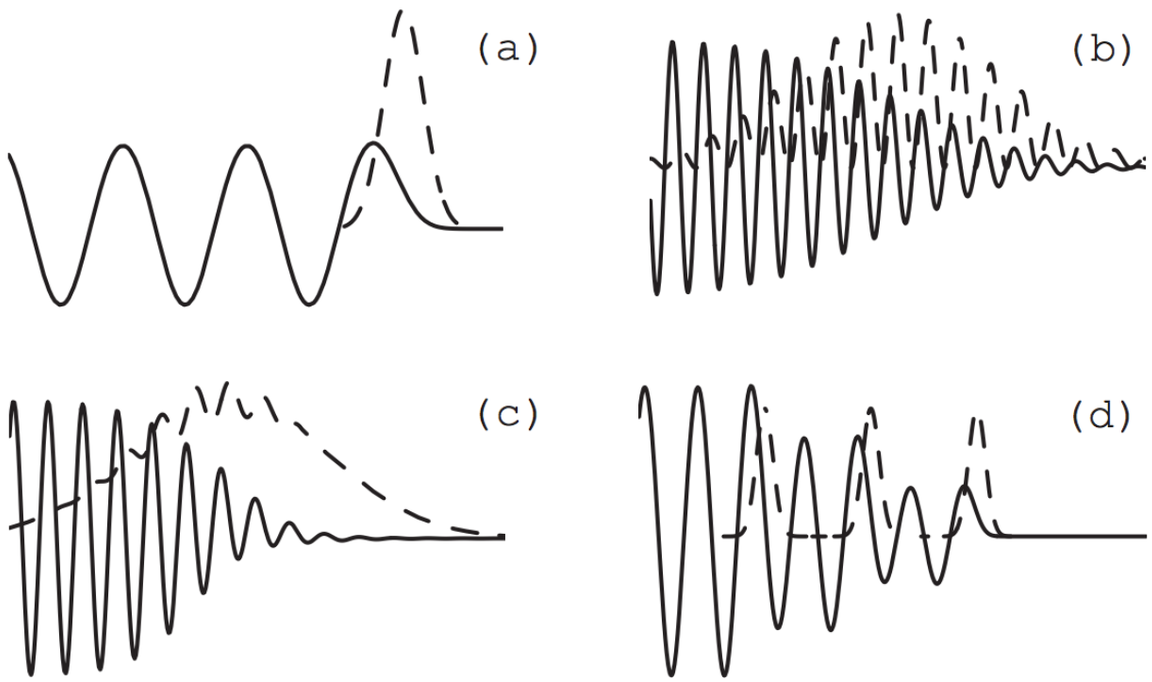

FIG. 1. Schematic of LPAs: (a) LWFA, (b) PBWA, (c) self-modulated (SM) LWFA, and (d) resonant laser pulse train. Shown are the excited plasma wave potentials (solid lines) and right-moving laser intensity envelopes (dashed lines).

Laser Driven PWA

Plasma-based accelerators are of great interest because of their ability to sustain extremely large acceleration gradients. The accelerating gradients in conventional radio-frequency (rf) linear accelerators (linacs) are currently limited to ~100 MV/m, partly due to breakdown that occurs on the walls of the structure. Ionized plasmas, however, can sustain electron plasma waves with electric fields in excess of $E_0 = cm_e\omega_p/e$ or

$$E_0(\mathrm{V/m}) \simeq 96\sqrt{n_0(\mathrm{cm}^{-3})}, \quad (1)$$

where $\omega_p = (4\pi n_0 e^2/m_e)^{1/2}$ is the electron plasma frequency, n_0 is the ambient electron number density, m_e and e are the electron rest mass and charge, respectively, and c is the speed of light in vacuum. Equation (1) is referred to as the cold nonrelativistic wave breaking field (Dawson, 1959). For example, a plasma density of $n_0 = 10^{18}$ cm^{-3} yields $E_0 \simeq 96$ GV/m, which is approximately three orders of magnitude greater than that obtained in conventional linacs. Accelerating gradients on the order of 100 GV/m have been inferred in plasma-based accelerator experiments (Gordon *et al.*, 1998; Malka *et al.*, 2002).

Beam Driven PWA

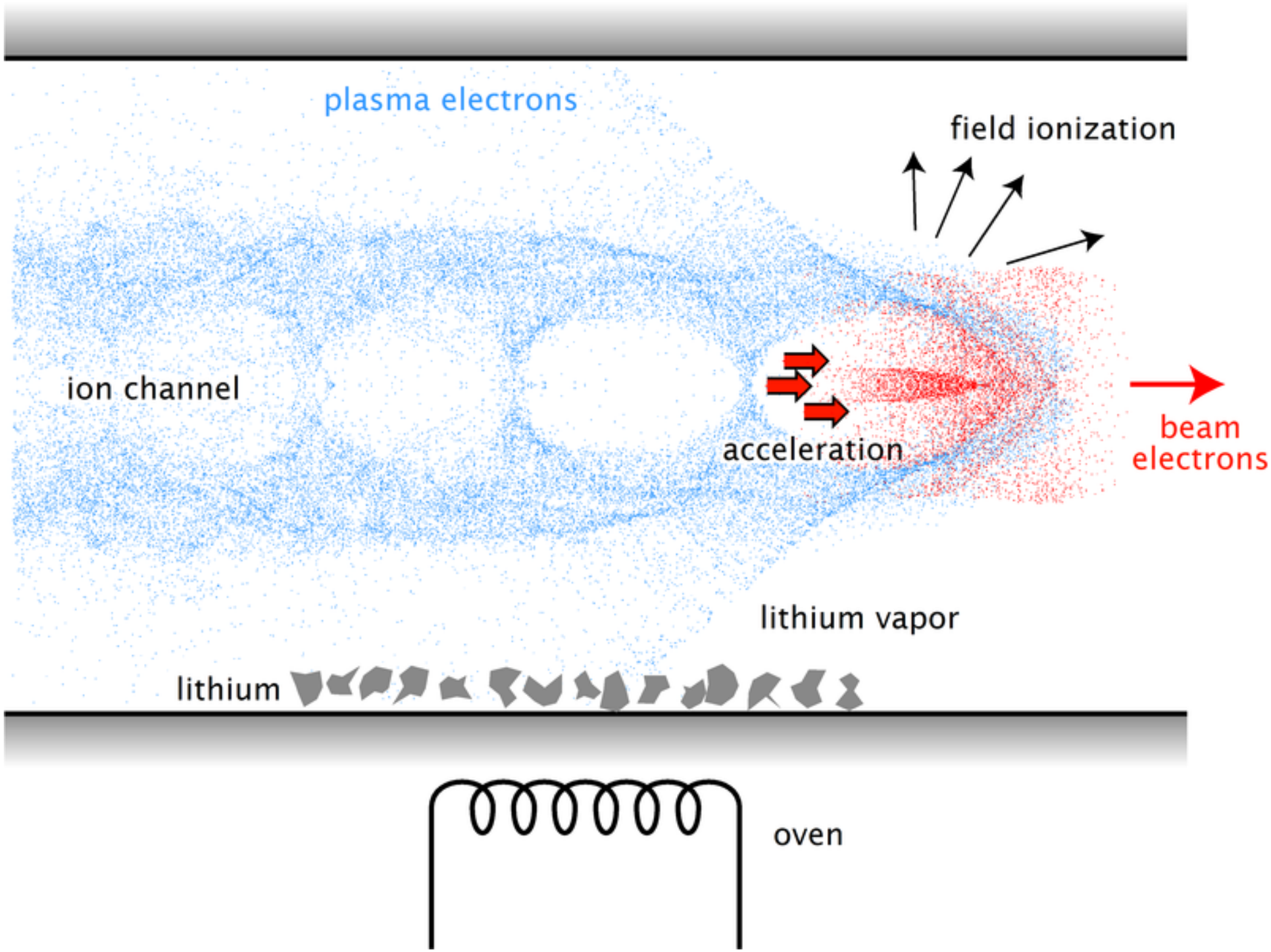

Illustration of the wake created by an electron beam in a plasma. This wake can be used to accelerate charged particles. Author: Rasmus Ischebeck.

Beam Driven PWA

Particle Accelerators, 1987, Vol. 22, pp. 81–99
Photocopying permitted by license only

Printed in the United States of America

BEAM LOADING IN PLASMA ACCELERATORS

T. KATSOULEAS, S. WILKS, P. CHEN,† J. M. DAWSON and J. J. SU
Department of Physics, University of California, Los Angeles, CA 90024

(Received April 21, 1986; in final form September 25, 1986)

We address the issue of beam loading in the plasma beat-wave and plasma wake-field accelerator schemes. We find the total number of particles which can be accelerated and the resulting efficiency subject to constraints on emittance growth and energy spread. The analytic predictions are compared to 1-D computer simulations.

The Wakefield Response in a 3D Cold Plasma

The wakefield generated by a relativistic charged-particle bunch of arbitrary shape

The Wakefield Generated By a Relativistic Charged-Particle Bunch of Arbitrary Shape.

(1)

$$\varepsilon_0 = q\,\delta(\vec{X} - \vec{V}_b t) = q\,\delta(\vec{r})\,\delta(z - V_b t)$$

$$\delta(\vec{r}) = \frac{1}{2\pi\sigma}\,\delta r$$

r is the radial polar coordinate

- Electric field response of a cold plasma to a bunch of arbitrary charge moving at c can be found from the Green's function response to a single test charge

The Wakefield Response in a 3D Cold Plasma

The wakefield generated by a relativistic charged-particle bunch of arbitrary shape

Linearised eq. of motion $\frac{d\vec{V}}{dt} = -e\vec{E}/m$ (2)

Continuity $\frac{\partial n_1}{\partial t} + n_0 \vec{\nabla}.\vec{V} = 0$ (3)

Maxwell's Eq. $\vec{\nabla}.\vec{E} = -4\pi e n_1 + 4\pi \rho_0$ (4) Poisson's

$\vec{\nabla} \times \vec{E} = -\frac{1}{c}\frac{\partial \vec{B}}{\partial t}$ (5)

$\vec{\nabla} \times \vec{B} = \left(\frac{4\pi}{c}\right)\vec{j} + \frac{1}{c}\frac{\partial \vec{E}}{\partial t}$ (6) Ampére's

$n_0 \rightarrow$ background

$n_1 \rightarrow$ perturbed plasma density

$\vec{V}, \vec{E} \rightarrow$ perturbed velocity and E field of the plasma

The Wakefield Response in a 3D Cold Plasma

The wakefield generated by a relativistic charged-particle bunch of arbitrary shape

→ Take the first derivative of eq. 3

$$\frac{\partial^2 n_1}{\partial t^2} + n_0 \frac{\partial}{\partial t}\left(\vec{\nabla}.\vec{v}\right) = 0$$

$$\frac{\partial^2 n_1}{\partial t^2} + n_0 \vec{\nabla}.\left(\frac{\partial \vec{v}}{\partial t}\right) = 0 \qquad \frac{\partial^2 n_1}{\partial t^2} + n_0 \vec{\nabla}.\left(-e\vec{E}/m\right) = 0$$

$\frac{\partial \vec{v}}{\partial t} = -e\vec{E}/m$

The Wakefield Response in a 3D Cold Plasma

The wakefield generated by a relativistic charged-particle bunch of arbitrary shape

→ Substitute $\vec{\nabla}.\vec{E}$ with Poisson's (eq. 4)

$$\frac{\partial^2 n_1}{\partial t^2} + \frac{n_0 e}{m}\left(-4\pi e n_1 + 4\pi \varrho_0\right) = 0$$

$$\frac{\partial^2 n_1}{\partial t^2} + \frac{n_0 e^2 n_1 4\pi}{m} - \frac{4\pi n_0 e \varrho_0}{m} = 0$$

$$\omega_p = \sqrt{\frac{4\pi n_0 e^2}{m}}$$

The Wakefield Response in a 3D Cold Plasma

The wakefield generated by a relativistic charged-particle bunch of arbitrary shape

$$\frac{\partial^2 n_1}{\partial t^2} + n_1 \omega_p^2 - (4\pi e_0)(n_0 e/m) = 0$$

$$\downarrow$$

$$q\,\delta(\vec{x} - \vec{V}_b t) = q\,\delta(\vec{r})\,\delta(z - V_b t)$$

$$\delta(z - V_b t) = \delta(t - z/V_b)/V_b$$

$$\hookrightarrow \frac{\partial^2 n_1}{\partial t^2} + n_1 \omega_p^2 = \underbrace{(4\pi e^2 n_0/m)}_{\omega_p^2}\,(q/e)\,\delta(\vec{r})\,\delta(t - z/V_b)/V_b$$

Wave equation for the plasma density response:

(7) $$\frac{\partial^2 n_1}{\partial t^2} + n_1 \omega_p^2 = \omega_p^2\,(q/e)\,\delta(\vec{r})\,\delta(t - z/V_b)/V_b$$

The Wakefield Response in a 3D Cold Plasma

The wakefield generated by a relativistic charged-particle bunch of arbitrary shape

→ Solution to eq. 7 is the Green's function for a harmonic oscillator:

(8) $$\left[n_1 = [\omega_p q \delta(\vec{r})/v_b e] \sin\left(\omega_p (t - z/v_b)\right) \theta(t - z/v_b) \right]$$

θ → step function (0 or 1) for pos. and neg. values of its argument.

The Wakefield Response in a 3D Cold Plasma

The wakefield generated by a relativistic charged-particle bunch of arbitrary shape

→ Curl of Eq. 5

$$\vec{\nabla}\times(\vec{\nabla}\times\vec{E}) = \vec{\nabla}\times\left(-\frac{1}{c}\frac{\partial\vec{B}}{\partial t}\right)$$

note: $\vec{\nabla}\times\vec{\nabla}\times\vec{A} = \vec{\nabla}(\vec{\nabla}\cdot\vec{A}) - \vec{\nabla}^2\vec{A}$

$$\vec{\nabla}\times(\vec{\nabla}\times\vec{E}) = \vec{\nabla}(\vec{\nabla}\cdot\vec{E}) - \vec{\nabla}^2\vec{E}$$

$$\vec{\nabla}(\vec{\nabla}\cdot\vec{E}) - \vec{\nabla}^2\vec{E} = -\frac{1}{c}\frac{\partial}{\partial t}(\vec{\nabla}\times\vec{B})$$

$$= -\frac{1}{c}\frac{\partial}{\partial t}\left(\frac{4\pi}{c}\vec{j} + \frac{1}{c}\frac{\partial\vec{E}}{\partial t}\right)$$

The Wakefield Response in a 3D Cold Plasma

The wakefield generated by a relativistic charged-particle bunch of arbitrary shape

$$\vec{\nabla}\cdot(\vec{\nabla}\cdot\vec{E}) - \vec{\nabla}^2\vec{E} = -\frac{4\pi}{c^2}\frac{\partial\vec{j}}{\partial t} - \frac{1}{c^2}\frac{\partial^2\vec{E}}{\partial t^2}$$

(9) $$\left(\frac{\partial^2}{\partial t^2} - c^2\vec{\nabla}^2\right)\vec{E} = -4\pi\frac{\partial\vec{j}}{\partial t} - c^2\vec{\nabla}(\vec{\nabla}\cdot E)$$

use
- Maxwell eq. $\rightarrow \vec{\nabla}\cdot\vec{E} = -4\pi\rho$
- continuity
- plasma density

Note: $\vec{j} = \frac{Q\vec{r}}{t} = Q\vec{v}$ $\quad \frac{\partial\vec{j}}{\partial t} = -n_0 e\frac{\partial\vec{V}}{\partial t} = n_0 e^2\vec{E}/m$

The Wakefield Response in a 3D Cold Plasma

The wakefield generated by a relativistic charged-particle bunch of arbitrary shape

$$(9)\quad \left(\frac{\partial^2}{\partial t^2} - c^2\vec{\nabla}^2\right)\vec{E} = -4\pi\frac{\partial \vec{j}}{\partial t} - c^2\vec{\nabla}(\vec{\nabla}\cdot\vec{E})$$

$$\frac{\partial \vec{j}}{\partial t} = n_0 e^2 \vec{E}/m$$

$$= -4\pi n_0 e^2/m\,\vec{E} - c^2\vec{\nabla}(\vec{\nabla}\cdot\vec{E})$$

$$\omega_p^2 \qquad -4\pi e n_1$$

$$= -\omega_p^2\vec{E} - c^2\vec{\nabla}\left(-4\pi e\,\omega_p\, q\,\delta(\vec{r})/V_b e\,\sin\left(\omega_p(t - z/V_b)\right)\Theta(t - z/V_b)\right)$$

$$= -\omega_p^2\vec{E} - c^2\vec{\nabla}\left(-4\pi\,\omega_p\, q/V_b\;\delta(\vec{r})\sin\left(\omega_p(t - z/V_b)\right)\Theta(t - z/V_b)\right)$$

The Wakefield Response in a 3D Cold Plasma

The wakefield generated by a relativistic charged-particle bunch of arbitrary shape

Note: • ∇^2 can be seperated into $\nabla_\perp^2 + \partial^2/\partial z^2$

• assume that z,t dependence of wakefields is a function of only the combination of $(z - V_b t) \cong (z - ct)$

i.e., $\partial^2/\partial t^2 = c^2 (\partial^2/\partial z^2)$

$$\left(c^2 \frac{\partial^2}{\partial z^2} - c^2 \nabla_\perp^2 - c^2 \frac{\partial^2}{\partial z^2} \right) \vec{E} = -\omega_p^2 \vec{E} - c^2 \vec{\nabla}(\dots)$$

$$-\nabla_\perp^2 \vec{E} = -\underbrace{\omega_p^2/c^2}_{k_p^2} \vec{E} - \vec{\nabla}(\dots)$$

$$k_p^2 = \omega_p^2/c^2$$

$$(\nabla_\perp^2 - k_p^2) \vec{E} = \vec{\nabla}(\dots)$$

The Wakefield Response in a 3D Cold Plasma

The wakefield generated by a relativistic charged-particle bunch of arbitrary shape

$\mathcal{L}$ ⟹

For longitudinal wake field E_z:

$$\left(\vec{\nabla}_\perp^2 - k_p^2\right)\vec{E}_z = 4\pi q k_p^2\, S(\vec{r})\,\theta(t-z/c)\cos\omega_p(t-z/c) \qquad (10)$$

Radial dependence of E_z is → Green's function response to the Helmholtz-Kelvin equation; that is:

$$E_z = -2q k_p^2 K_0(k_p r)\,\theta(t-z/c)\cos\omega_p(t-z/c) \qquad (11)$$

K_0 → zeroth-order Bessel function of the second kind.

The Wakefield Response in a 3D Cold Plasma

The wakefield generated by a relativistic charged-particle bunch of arbitrary shape

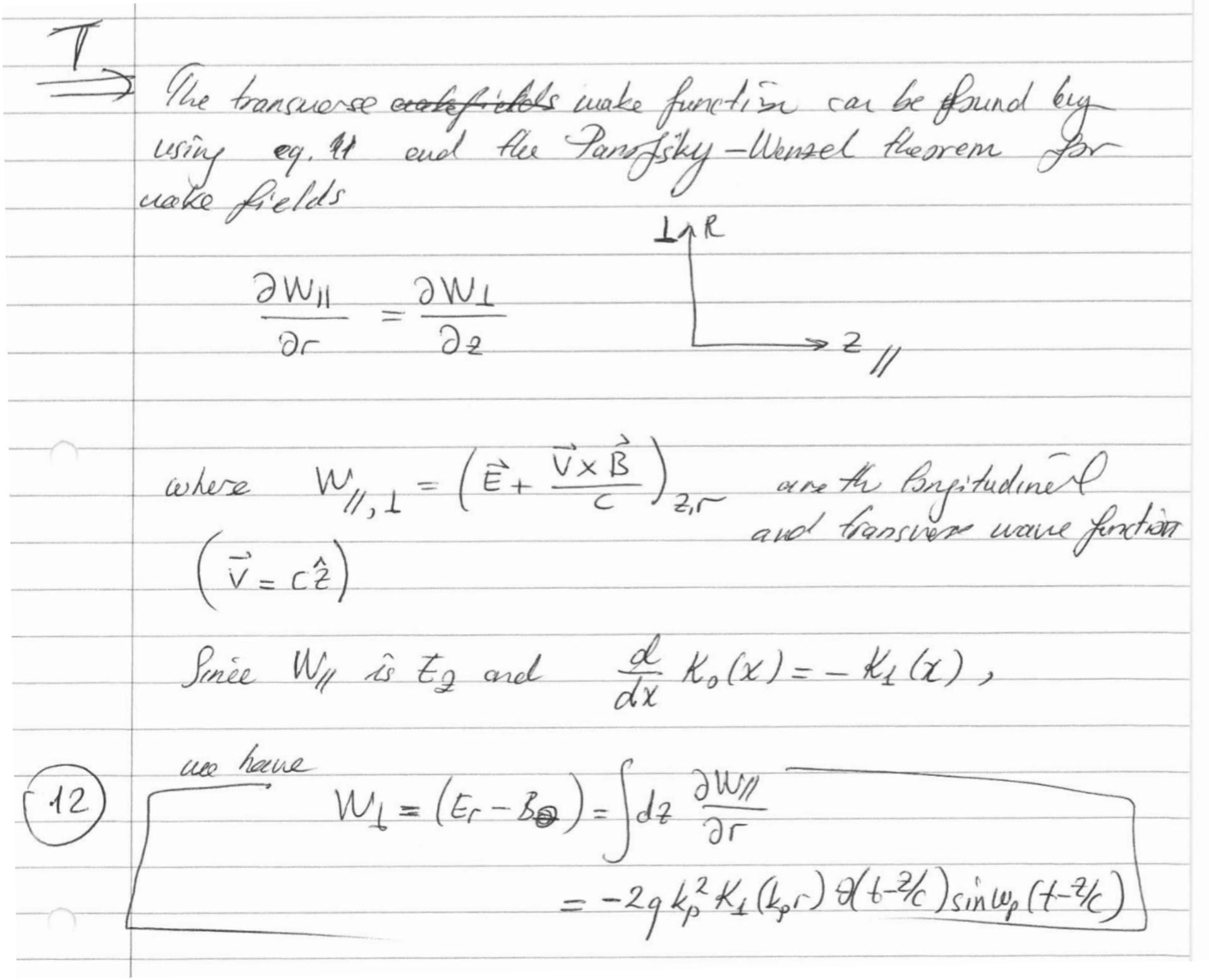

The transverse ~~wakefields~~ wake function can be found by using eq. 11 and the Panofsky–Wenzel theorem for wake fields

$$\frac{\partial W_{\parallel}}{\partial r} = \frac{\partial W_{\perp}}{\partial z}$$

where $W_{\parallel,\perp} = \left(\vec{E} + \frac{\vec{v}\times\vec{B}}{c}\right)_{z,r}$ are the longitudinal and transverse wave function

$\left(\vec{v} = c\hat{z}\right)$

Since $W_{\parallel}$ is E_z and $\frac{d}{dx}K_0(x) = -K_1(x)$,

(12) we have

$$W_{\perp} = (E_r - B_\theta) = \int dz \frac{\partial W_{\parallel}}{\partial r}$$

$$= -2q k_p^2 K_1(k_p r)\, \theta(t - z/c) \sin\omega_p (t - z/c)$$

The Wakefield Response in a 3D Cold Plasma

The wakefield generated by a relativistic charged-particle bunch of arbitrary shape

Eq. 11 and 12 defines the wake fields produced behind a single charge.

→ Wakefield produced by an arbitrary charge distribution with the density of:

$\varrho_b(r, \theta, z-ct)$

→ Put ϱ_b into equations and integrate.

→ Consider different bunch density profiles (optimise beams energy spread through beam loading)

→ Incorporate plasma density profile?

in practical units…

- Doğrusal kuram için ($n_b > n_p$) elde edilebilecek en yüksek elektrik alan:

$$E = 240(MV/m)(\frac{N}{4\times10^{10}})(\frac{0.6}{\sigma_z(mm)})^2$$

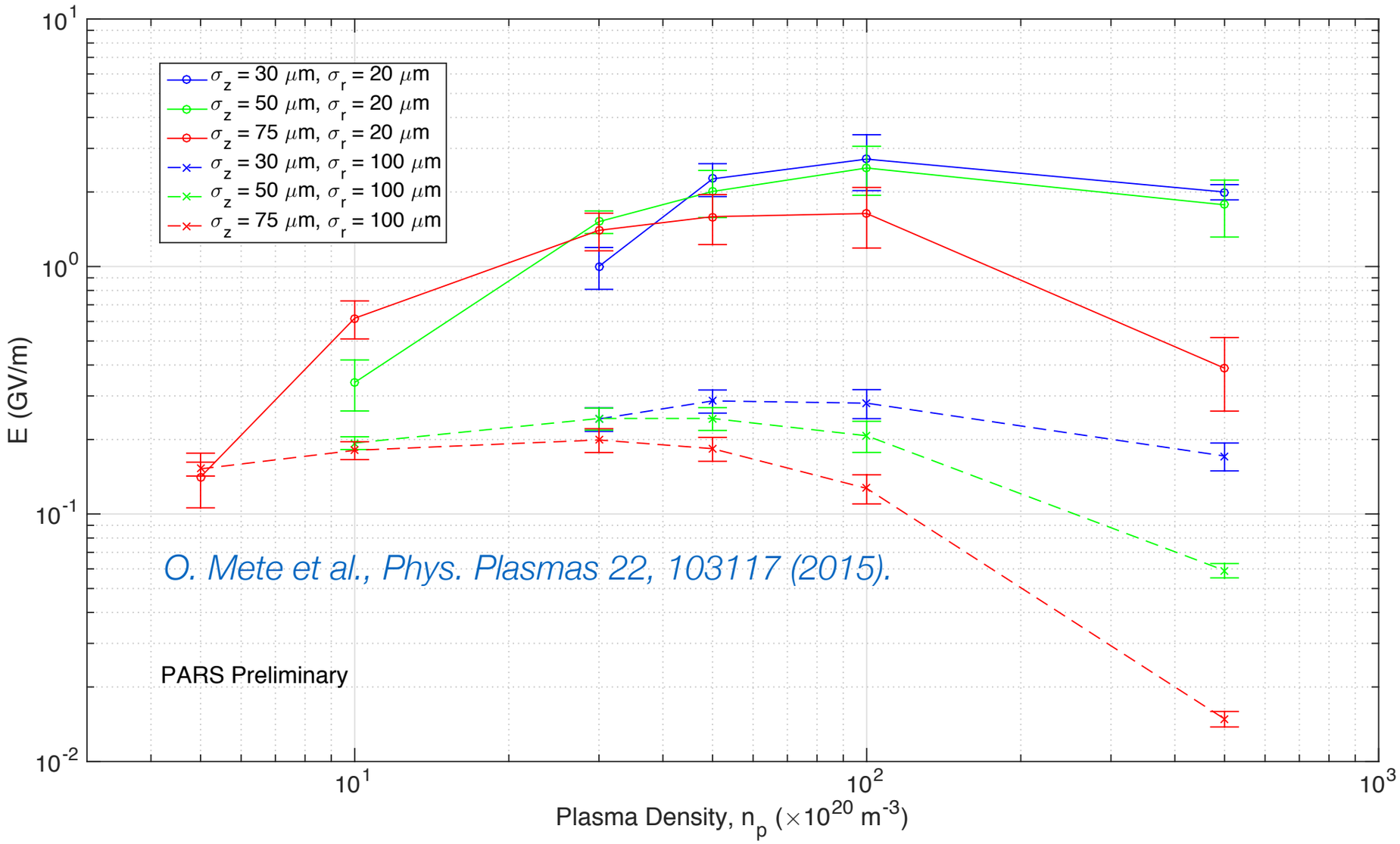

in practical units…

- Dönüşüm oranı, sürücü demetten tanık demete aktarılabilecek en büyük enerji:

$$R = E_+ / E_-$$

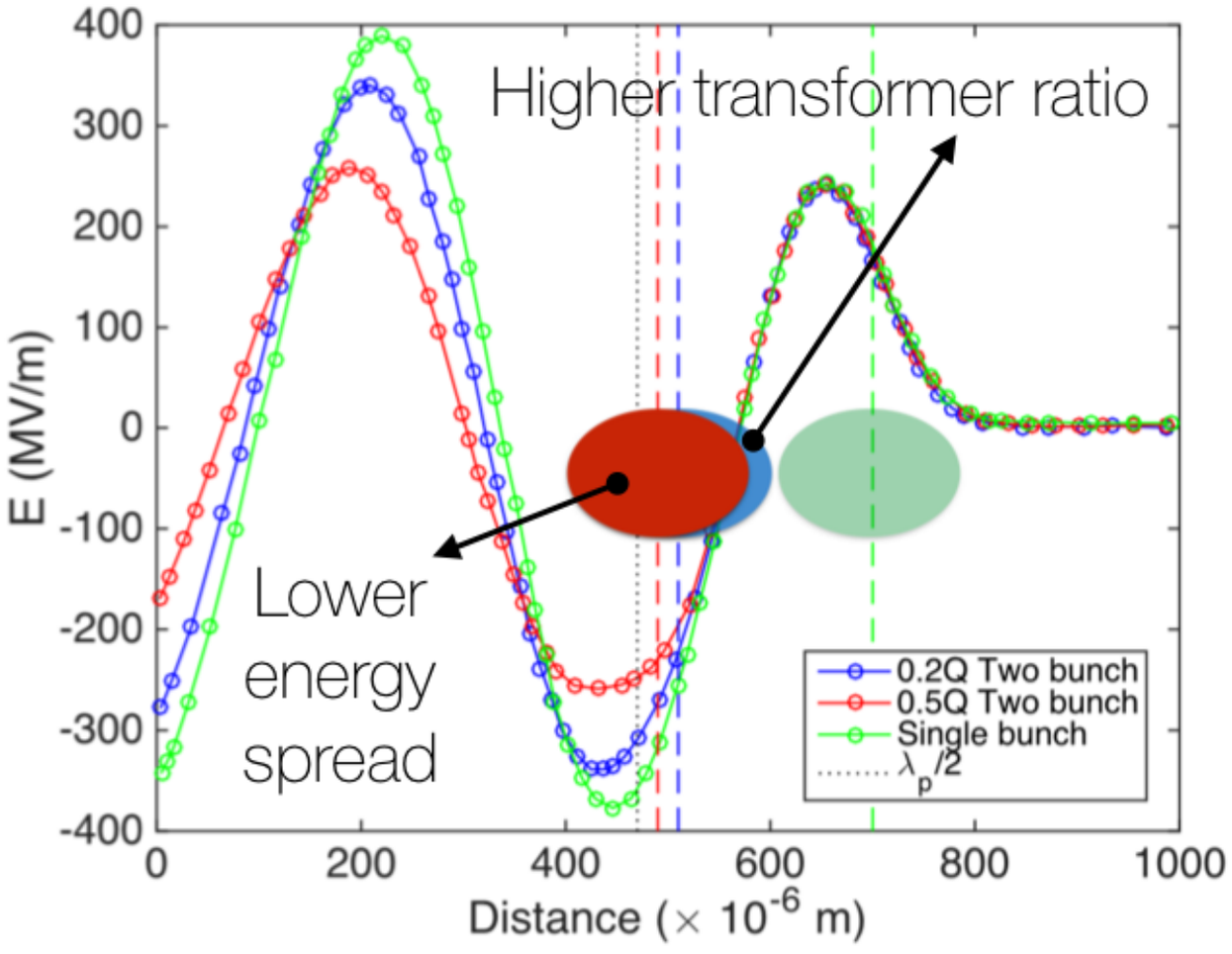

O. Mete et al., Phys. Plasmas 22, 103117 (2015).

Proton Driven PWA and Self Modulation Instability

A. Caldwell and K. V. Lotov, Phys. Plasmas 18, 103101 (2011); doi: 10.1063/1.3641973

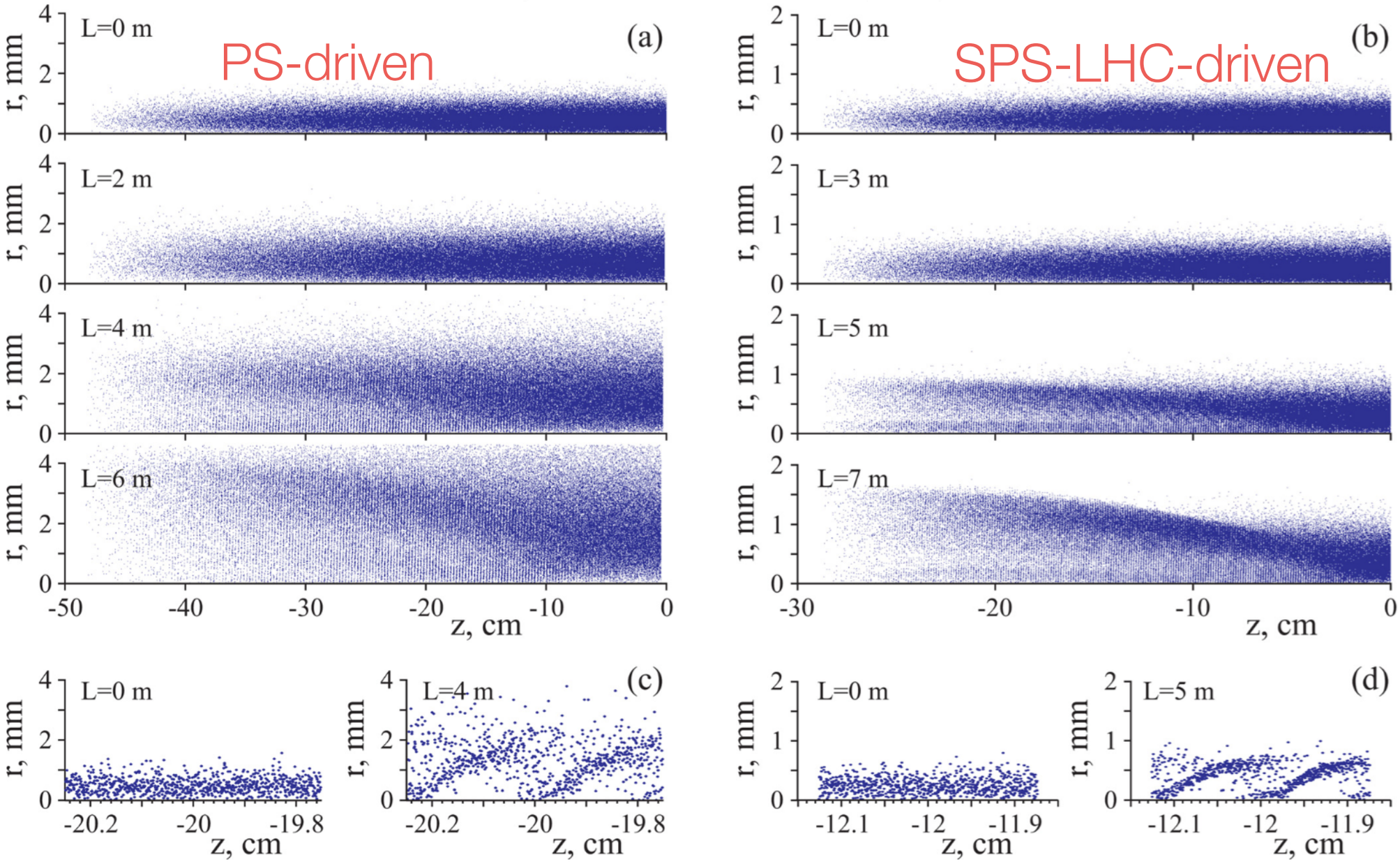

FIG. 1. (Color online) Bunch portraits at different propagation lengths showing the part of the bunch traveling in the plasma (a, b) and the zoomed area located $\approx\sigma_z$ behind the bunch center (c, d) for the PS bunch (left) and SPS-LHC bunch (right).

- Seeded - Proton bunch co-propagates with ionising laser.
- nb/np ~ 0.3%, no wave breaking, fluid approximation is valid.

Proton Driven PWA and Self Modulation Instability

A. Caldwell and K. V. Lotov, Phys. Plasmas 18, 103101 (2011); doi: 10.1063/1.3641973

$$n_P = \frac{N_P}{2\sigma_r^2\sigma_z(2\pi)^{3/2}} e^{-r^2/2\sigma_r^2}\left[1 + cos\left(\sqrt{\frac{\pi}{2}}\frac{z}{\sigma_z}\right)\right]$$ Initial proton beam profile.

$\sigma_{z,0}k_p \gg 1$ Initial driver bunch length much larger than the plasma wavelength.

$N_e \approx 0.3\xi^{2/3}\tau^{1/3}$ Number of e-foldings in units of: k_p^{-1} c/ω_b

$$\omega_b = \sqrt{\frac{4\pi n_b e^2}{\gamma_b M}}$$ Bunch modulation frequency.

$$n_b = \frac{N}{(2\pi)^{3/2}\sigma_r^2\sigma_z}$$ Density in the central part of the Gaussian bunch.

Proton Driven PWA and Self Modulation Instability

A. Caldwell and K. V. Lotov, Phys. Plasmas 18, 103101 (2011); doi: 10.1063/1.3641973

We now suppose we can reach the state where we have maximum modulation of the bunch and investigate the strength of the electric fields. The bunch has been divided into microbunches which each contains ≈1/2 of the initial number of protons within one plasma wavelength (the other protons are pushed out by the radial fields). We can use the expression in Sec. II to estimate the electric field from one microbunch

$$E_{\mu,\mathrm{z,max}} = eN_\mu Z(k_p,\sigma_z)R(k_p\sigma_r), \tag{8}$$

where N_μ is the number of protons in the microbunch and $\sigma_z \approx \sqrt{2}k_p^{-1}$ is the rms length of the protons in the microbunch. If we assume for seeded instabilities that all microbunches behind the center of the proton bunch add coherently to the produced electric field, then we have

$$E_{\mathrm{z,max}} \approx \frac{eN}{4} Z(k_p,\sigma_z)R(k_p\sigma_r)\ . \tag{9}$$

We now calculate the maximum electric field by taking $k_p\sigma_r = 1$, substituting $\sigma_z \approx \sqrt{2}k_p^{-1} = \sqrt{2}\sigma_r$ and using Eqs. (2) and (3). This yields

$$E_{\mathrm{z,max}} \approx 0.085\,\frac{Ne}{\sigma_r^2} \approx 0.12\ \mathrm{GV/m}\cdot\left(\frac{N}{10^{10}}\right)\left(\frac{100\ \mu\mathrm{m}}{\sigma_r}\right)^2. \tag{10}$$

Proton Driven PWA and Self Modulation Instability

A. Caldwell and K. V. Lotov, Phys. Plasmas 18, 103101 (2011); doi: 10.1063/1.3641973

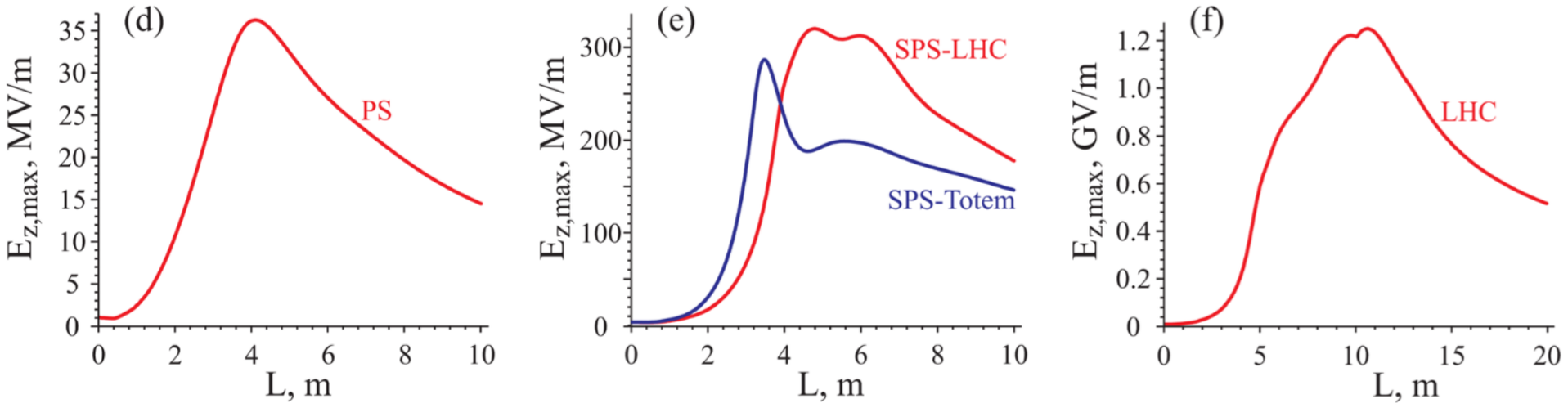

Plasma step-up:

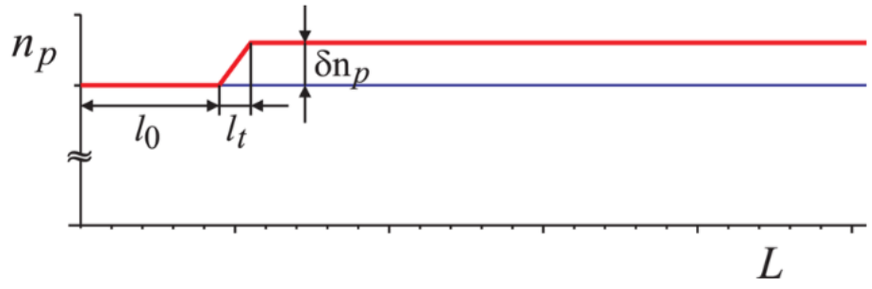

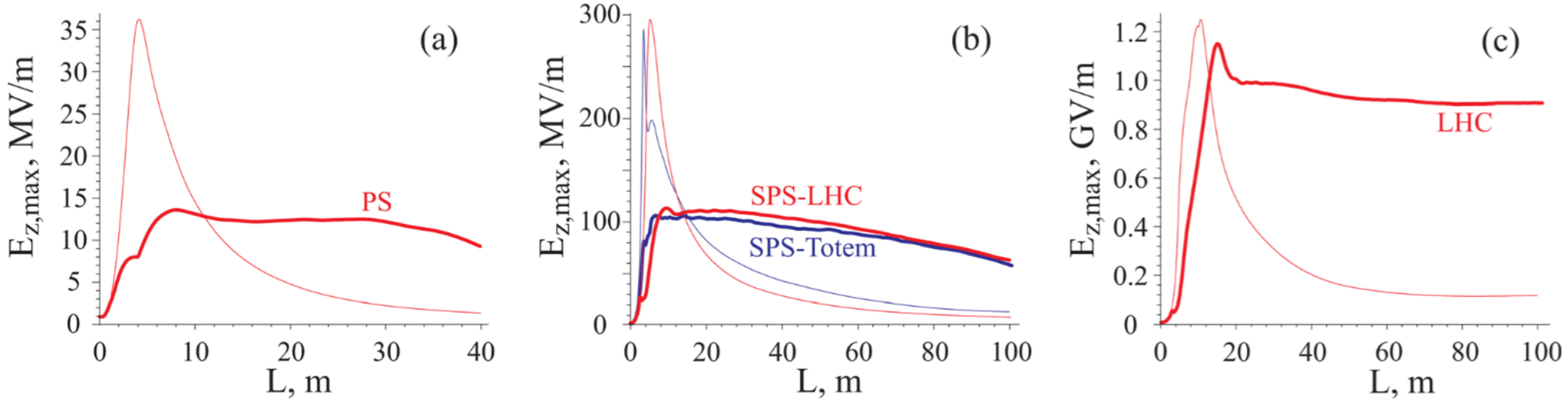

Positron Acceleration and Hollow Plasma Channel

Gessner et al., IPAC16, WEPMY030

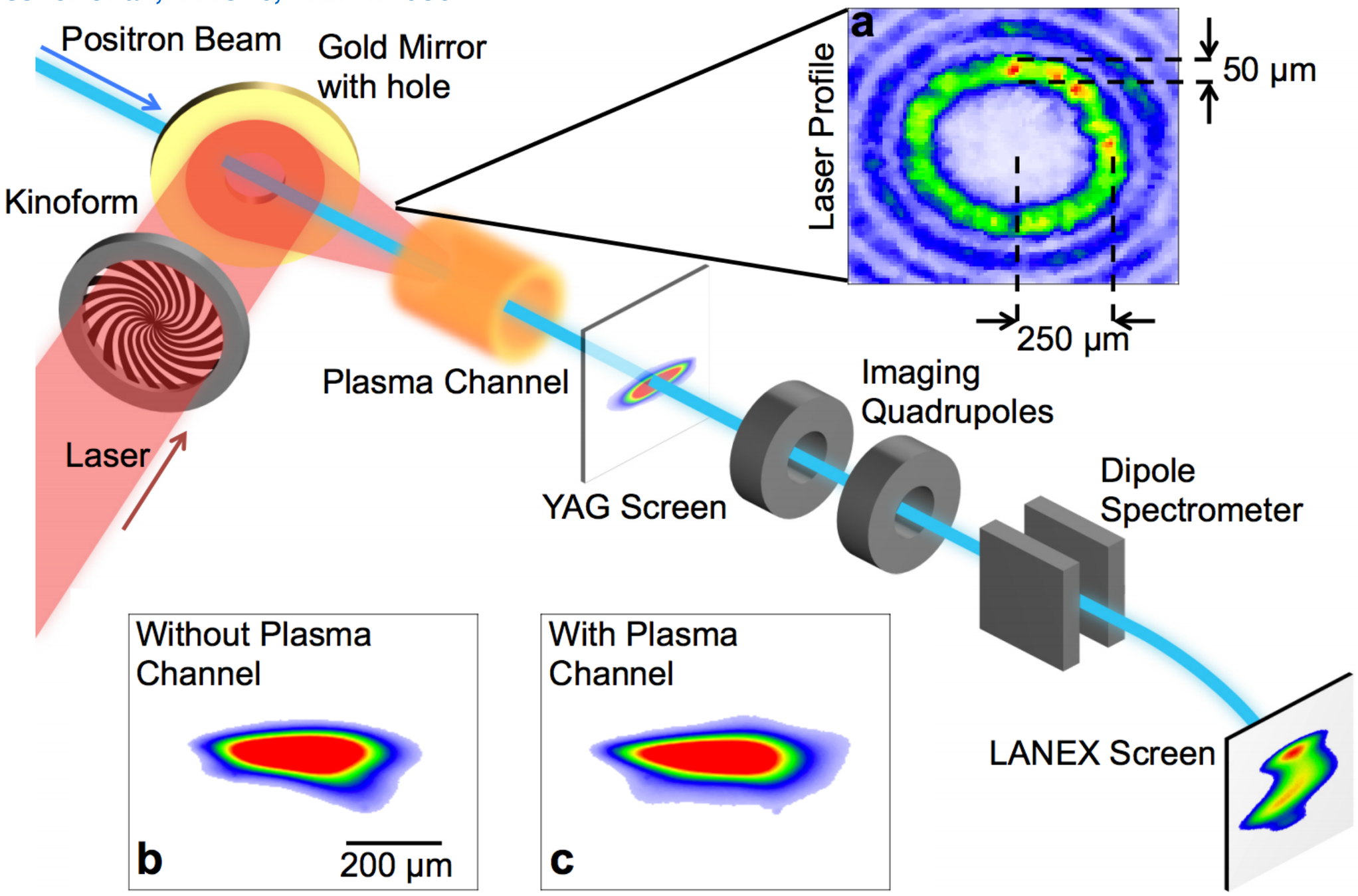

Hollow plasma concept: Kimura et al., PRSTAB 14, 041301 (2011).
Collider concept: Schroder et al., PRSTAB in press (2016), http://dx.doi.org/10.1016/j.nima.2016.03.001.

Positron Acceleration and Hollow Plasma Channel

Gessner et al., IPAC16, WEPMY030

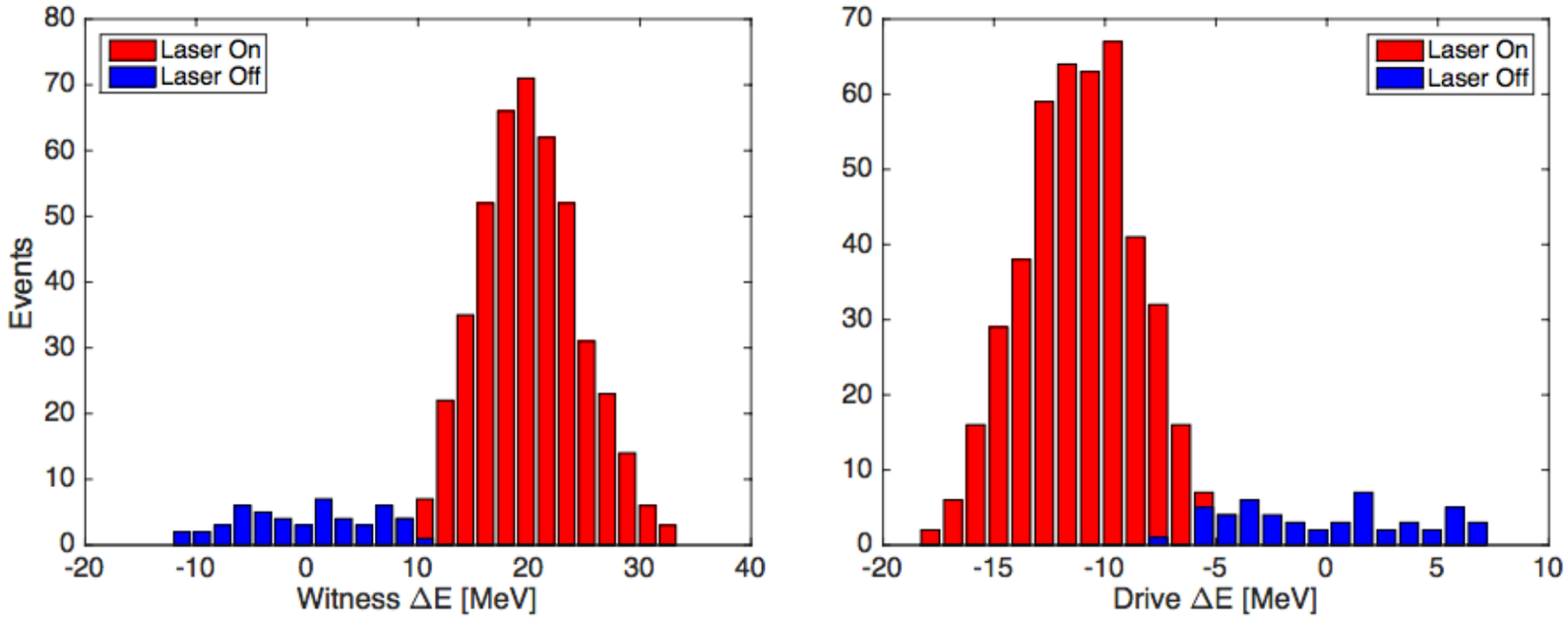

Figure 4: Left: The energy gain histogram for the witness bunch. The average energy gain is 19.9 MeV and the highest energy event is 33.4 MeV. Right: The energy loss histogram for the drive bunch. The average energy loss is 11 MeV. Note that in for this data, we operated with a 10 Hz positron beam and a 9 Hz laser, so that one out of every ten shots is a no-plasma background reference. There are 500 total shots in this dataset.

Hollow plasma concept: Kimura et al., PRSTAB 14, 041301 (2011).
Collider concept: Schroder et al., PRSTAB in press (2016), http://dx.doi.org/10.1016/j.nima.2016.03.001.

https://www.cockcroft.ac.uk/lectures

The Cockcroft Institute
of Accelerator Science and Technology

Type your keywords... Search

News | About » | People | Research » | Education » | Output » | Events | Join Us | Contacts

Lectures

Postgraduate Lecture Programme

A key goal of the Cockcroft Institute is to educate the next generation of particle accelerator scientists and engineers. As part of this goal the Cockcroft institute runs a 2 year postgraduate education programme in accelerator science and technology for both its own PhD students and for students at other universities. The lectures are all recorded to be webcast and archived and they are free to view for anyone via the institute website.

LIVE STREAM and ON DEMAND Cockcroft Webinar Portal

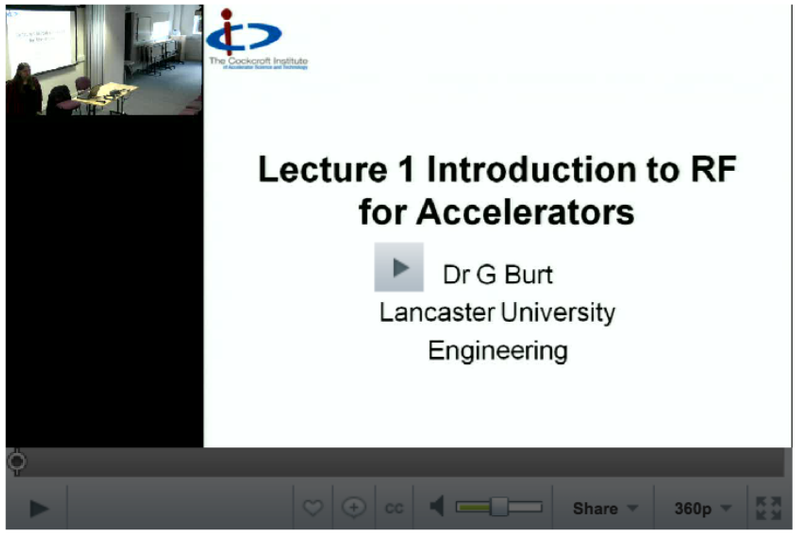

The programme has an initial 3 months introductory programme starting in October and runs every Monday morning until December. This covers the basics of accelerator science and technology, including beam dynamics and magnets. This is then followed by an advanced programme running on Monday mornings from January to September over two years covering topics such as Hamiltonian beam dynamics, free electron lasers, radio frequency engineering and laser plasma acceleration.

Recent News

- CI Research presented in the Land of the Morning Calm
- Quantum Sensors for Fundamental and Information Science
- Microwave suppression of surface resistance and dissipation limits in superconducting resonator cavities at strong RF fields.
- How would a laser plasma accelerator with industry beam quality look like?

News and Events Calendar

May 2016

M	T	W	T	F	S	S
						1
2	3	4	5	6	7	8
9	10	11	12	13	14	15
16	17	18	19	20	21	22
23	24	25	26	27	28	29
30	31					

« Apr

Lecture Slides available here

- Academic Training Programme 2015 - 2016
- Academic Training Programme 2014 - 2015
- Academic Training Programme 2013 - 2014
- Academic Training Programme 2012 - 2013
- Academic Training Programme 2011 - 2012
- Academic Training Programme 2010 - 2011
- Academic Training Programme 2009 - 2010
- Academic Training Programme 2008- 2009
- Academic Training Programme 2007- 2008
- Academic Training Programme 2006 - 2007
- Academic Training Programme 2005 - 2006
- Academic Training Programme 2004 - 2005

Thank you for your attention...